Supplementary Information

In situ synthesis of metal clusters encapsulated within small-pore zeolite via a dry gel conversion method

Xiaoli Yang,[ab] Qinggang Liu,[a] Yaru Zhang,[ab] Xiong Su,[*a] Yanqiang Huang[*ac] and Tao Zhang[ac]

[a] tate Key Laboratory of Catalysis, Dalian Institute of Chemical Physics, Chinese Academy of Sciences, No. 457 Zhongshan Road, Dalian 116023, P. R. China.

[b] University of Chinese Academy of Sciences, Beijing 100049, P. R. China.

[c] iChEM (Collaborative Innovation Center of Chemistry for Energy Materials), Dalian Institute of Chemical Physics, Chinese Academy of Sciences, Dalian 116023, P. R. China.

[*] Corresponding authors, E-mail: suxiong@dicp.ac.cn, yqhuang@dicp.ac.cn.

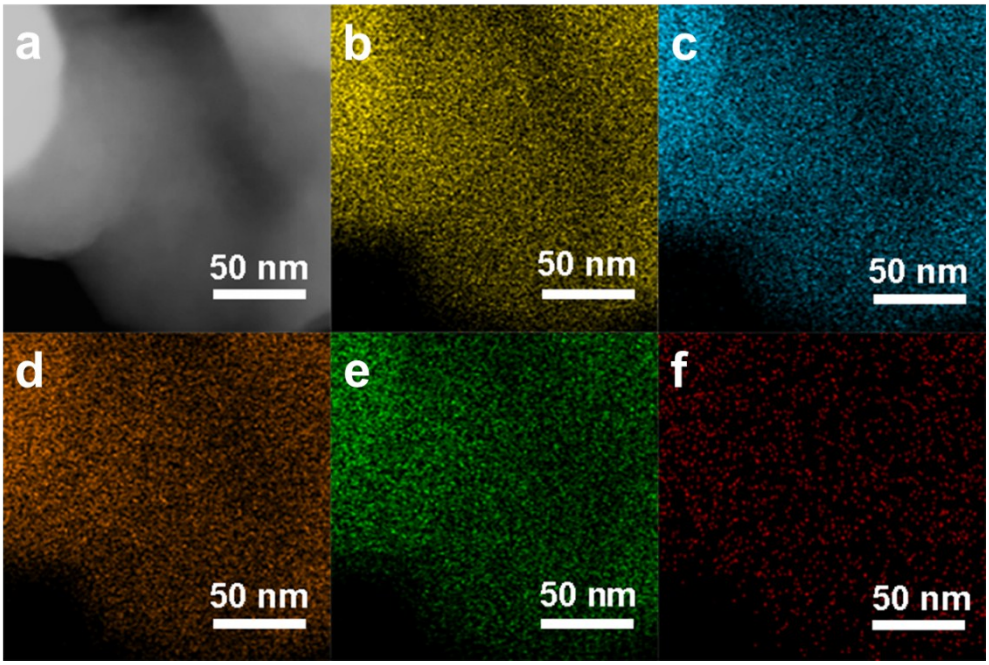

Fig. S1 Elemental maps for the Pt/Schiff-SiO_2 sample, (a) TEM image, (b) Si (yellow), (c) C (blue), (d) O (orange), (e) N (green), (f) Pt (red).

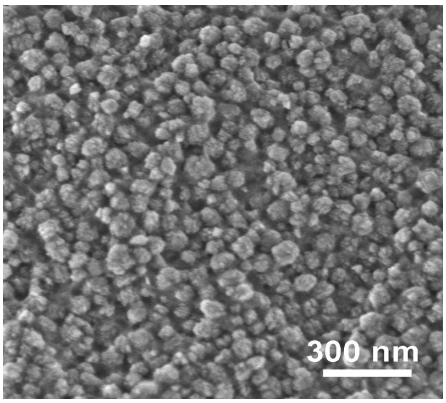

Fig. S2 SEM images of ZSM-5 seed.

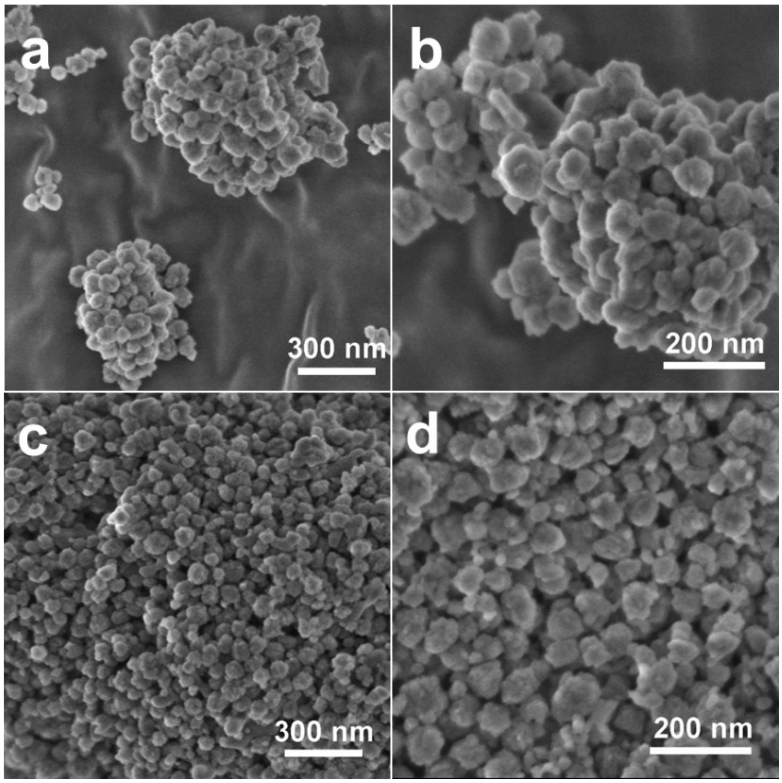

Fig. S3 SEM images of Pt@MFI-a (a-b) and Pt@MFI-b (c-d).

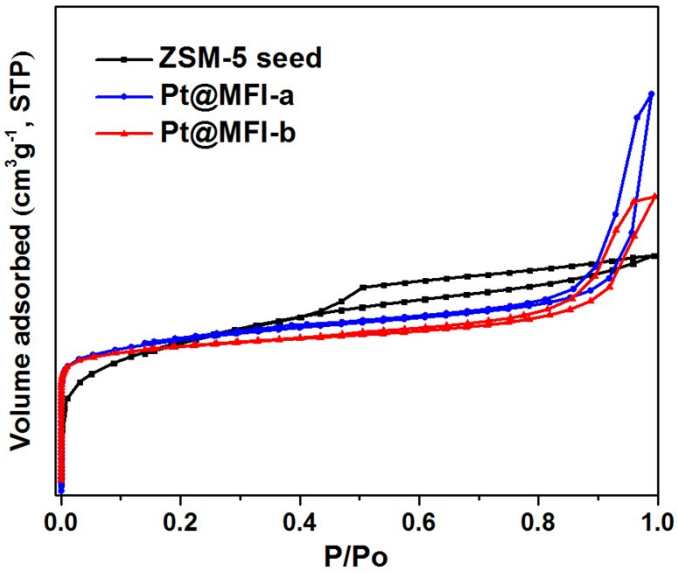

Fig. S4 N_2 adsorption-desorption isotherms of the samples.

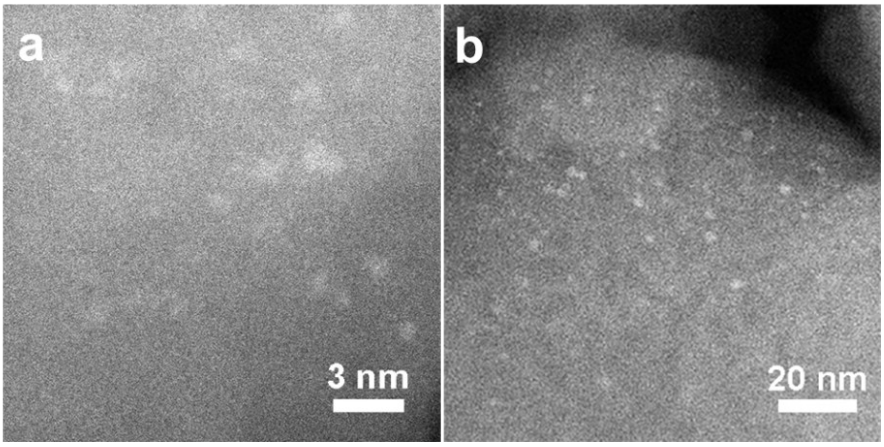

Fig. S5 STEM images of Pt@MFI-b after calcination at 500 °C with the scale bar of (a) 3 nm, (b) 20 nm.

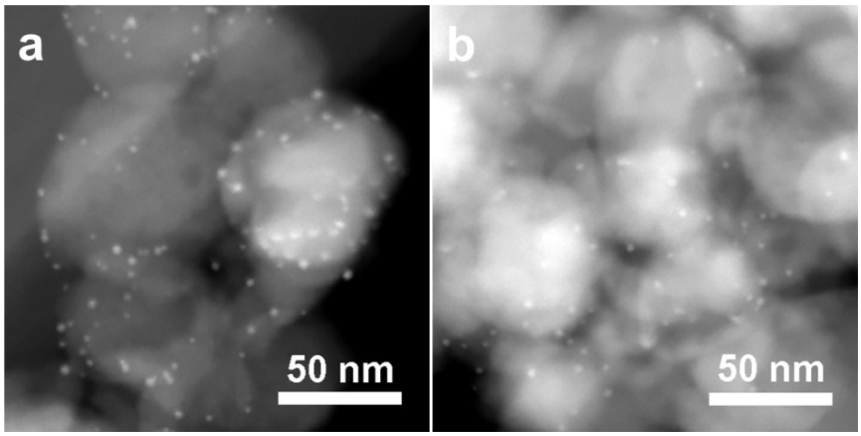

Fig. S6 STEM images of Pt@MFI-b after calcination at 800 °C.

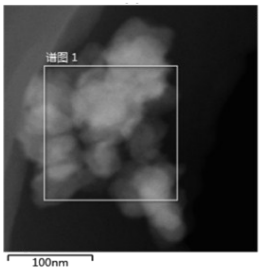

element	Line type	k factor	wt%	wt% Sigma
C	K	2.50675	45.99	1.08
O	K	1.86867	26.60	0.83
Si	K	1.00000	27.16	0.72
Pt	L	2.67312	0.24	0.24
total			100.00	

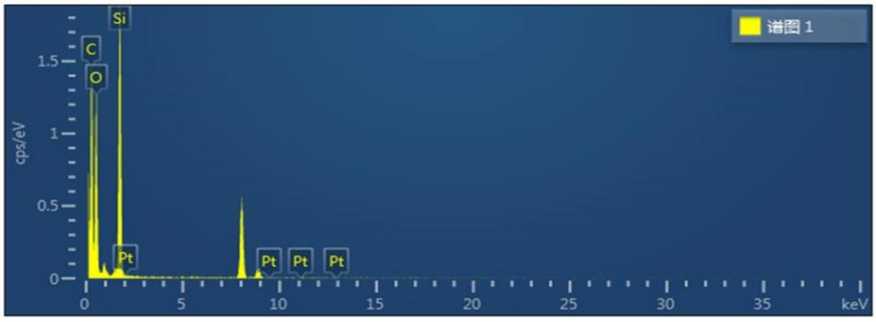

Fig. S7 EDS analysis of Pt@MFI-a without calcination.

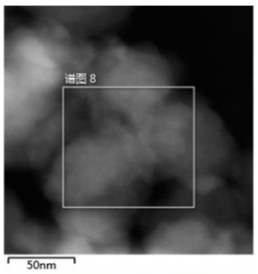

element	Line type	k factor	wt%	wt% Sigma
O	K	1.86867	30.80	2.07
Al	K	1.03564	0.33	0.78
Si	K	1.00000	67.84	2.22
Pt	L	2.67312	1.03	1.14
total			100.00	

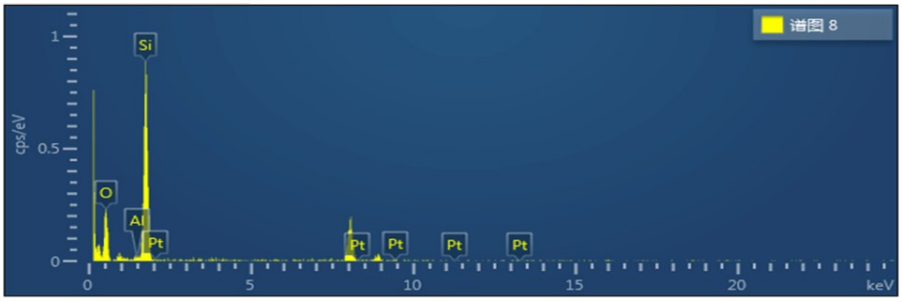

Fig. S8 EDS analysis of Pt@MFI-b without calcination.

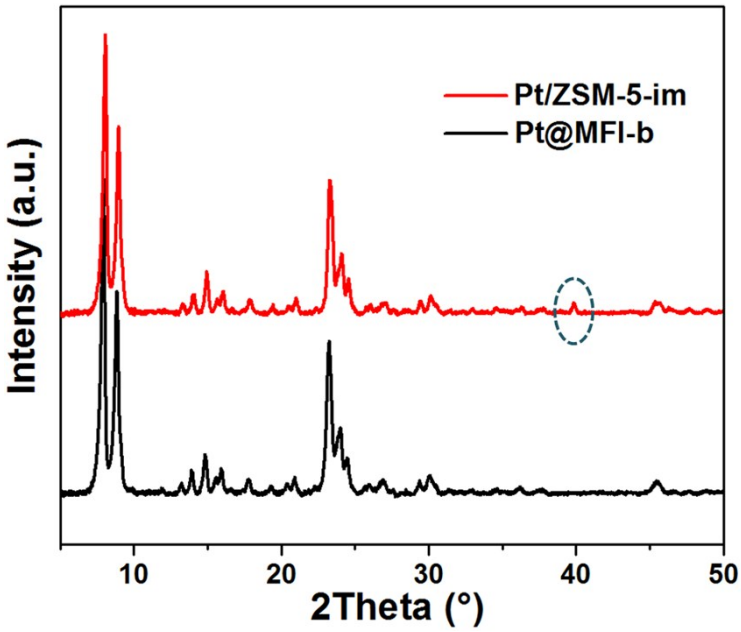

Fig. S9 XRD patterns of Pt/ZSM-5-im and Pt@MFI-b after calcination at 500 °C.

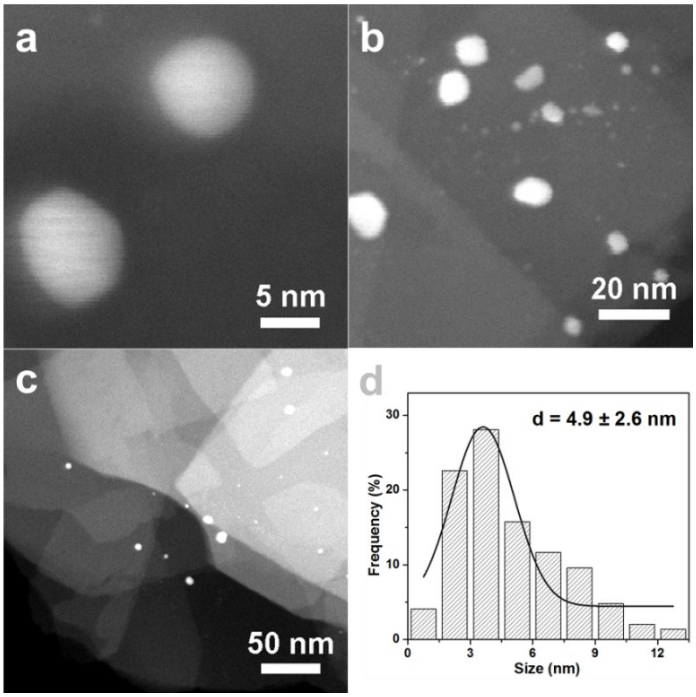

Fig. S10 STEM images of Pt/ZSM-5-im after calcination at 500 °C under the scale bar of (a) 5 nm, (b) 20 nm, (c) 50 nm, (d) the particle size distribution.

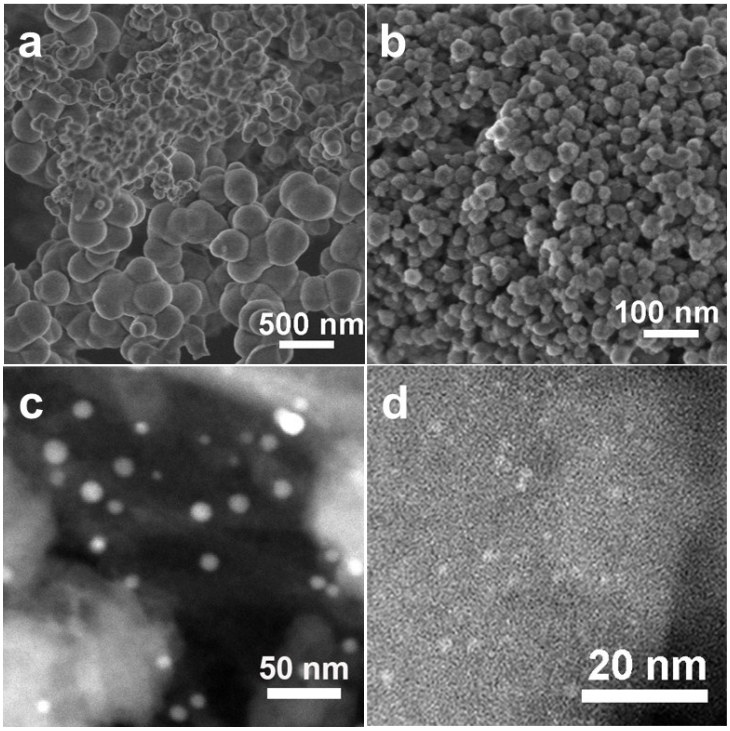

Fig. S11 SEM images of (a) Pt/Schiff-SiO_2&MFI-b and (b) Pt@MFI-b, the corresponding TEM images of (c) Pt/Schiff-SiO_2&MFI-b and (d) Pt@MFI-b after calcination at 500 °C.

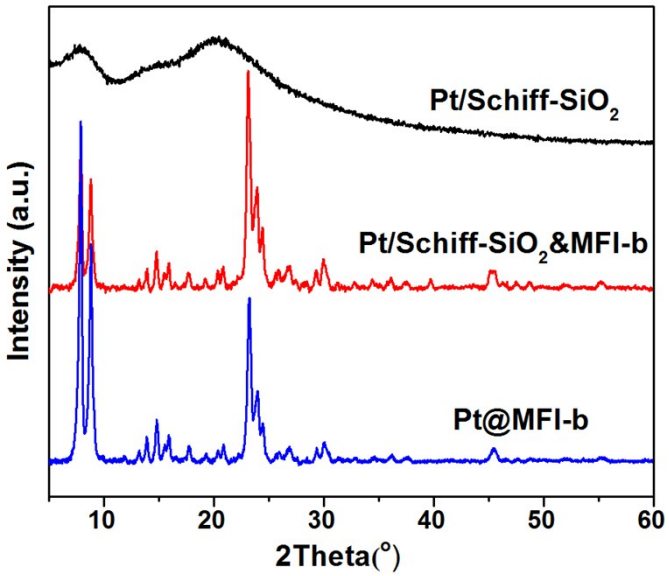

Fig. S12 XRD patterns of Pt/Schiff-SiO_2 before calcination, Pt/Schiff-SiO_2&MFI-b and Pt@MFI-b after calcination at 500 °C.

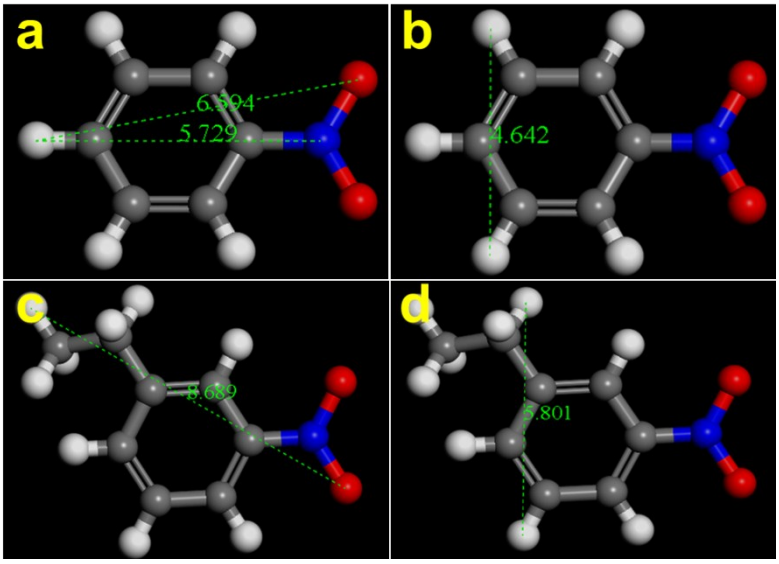

Fig. S13 The dynamic diameter of (a-b) nitrobenzene and (c-d) 3-nitrotoluene.

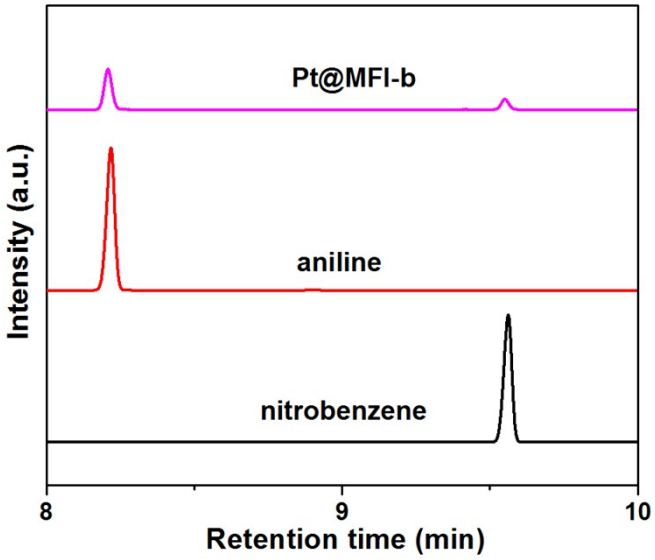

Fig. S14 Gas chromatogram of products after reduction of nitrobenzene over Pt@MFI-b catalysts and the corresponding standard samples.

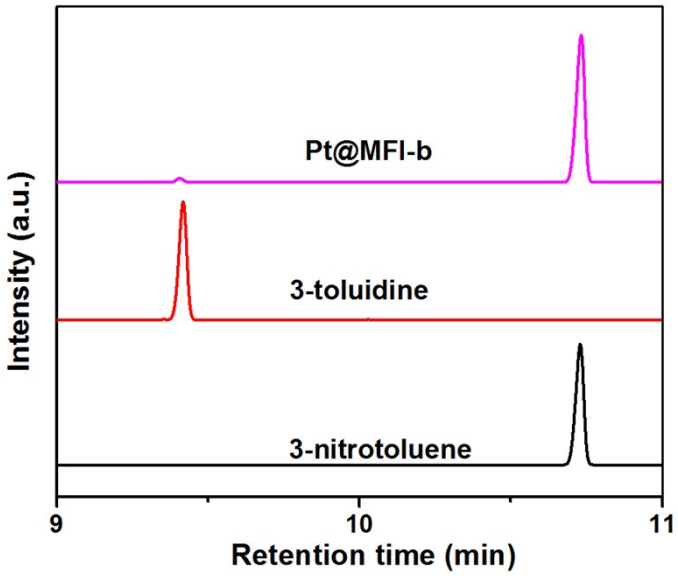

Fig. S15 Gas chromatogram of products after reduction of 3-nitrotoluene over Pt@MFI-b catalysts and the corresponding standard samples.

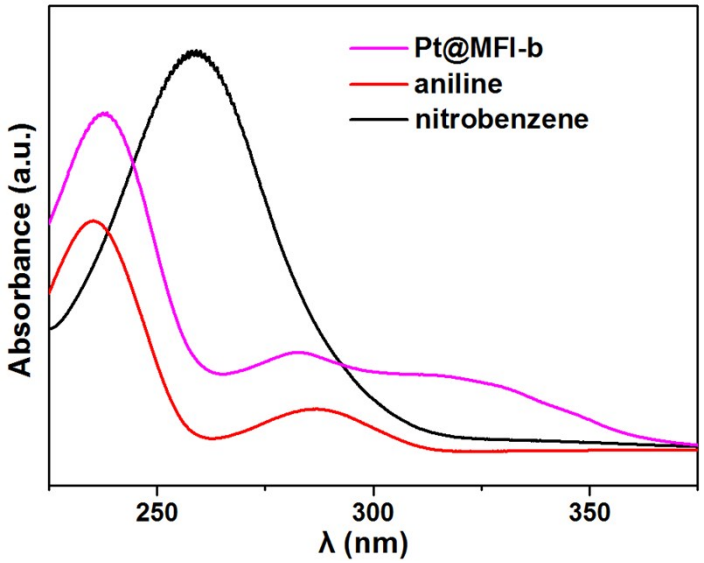

Fig. S16 UV-vis absorption spectra of products after reduction of nitrobenzene over Pt@MFI-b and the corresponding standard substances.

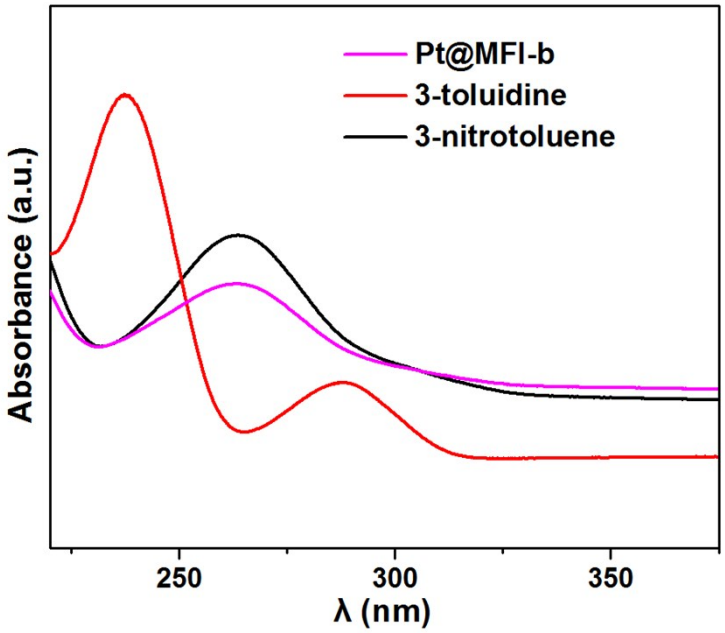

Fig. S17 UV-vis absorption spectra of products after reduction of 3-nitrotoluene over Pt@MFI-b and the corresponding standard substances.

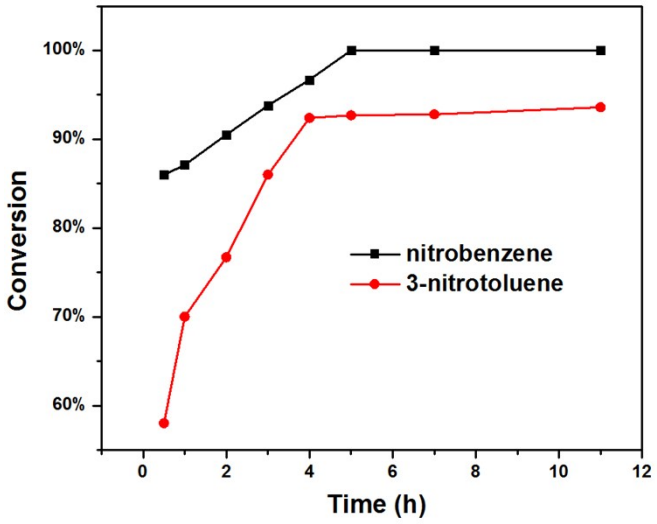

Fig. S18 The hydrogenation of nitrobenzene and 3-nitrotoluene over Pt@MFI-b catalyst.

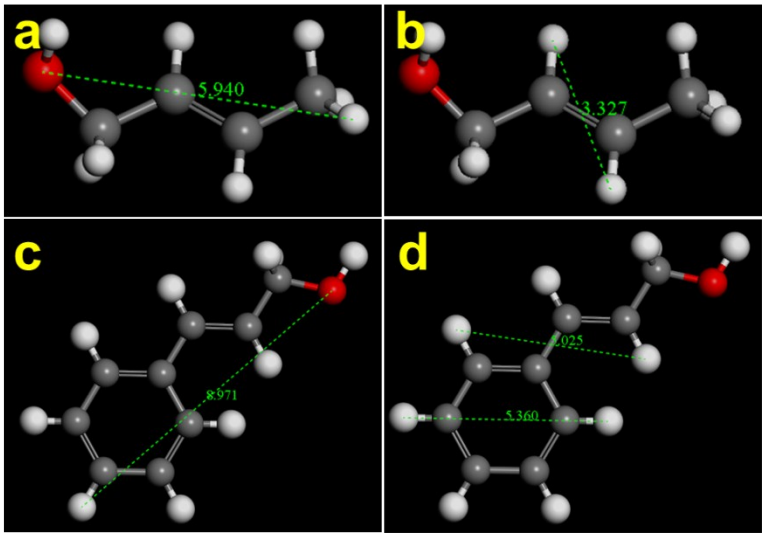

Fig. S19 The dynamic diameter of (a-b) croton alcohol and (c-d) cinnamyl alcohol.

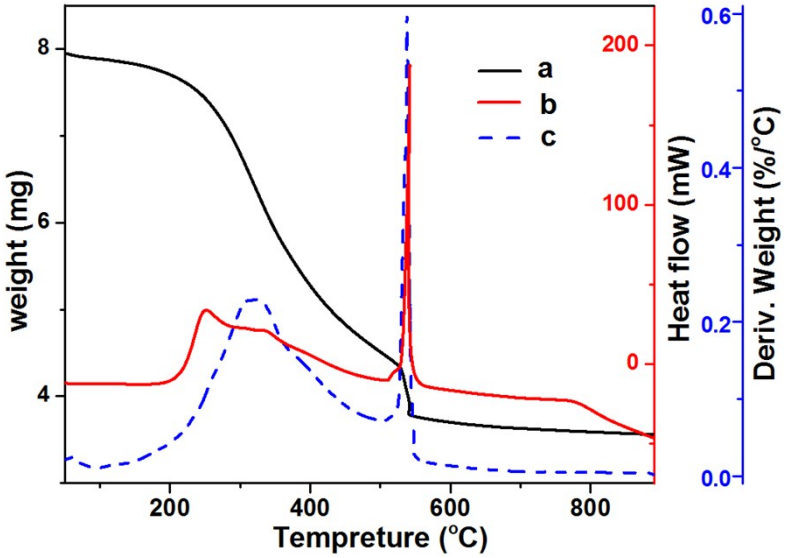

Fig. S20 (a) TG, (b) DTA and (c) DTG curves of Pt/Schiff-SiO_2.

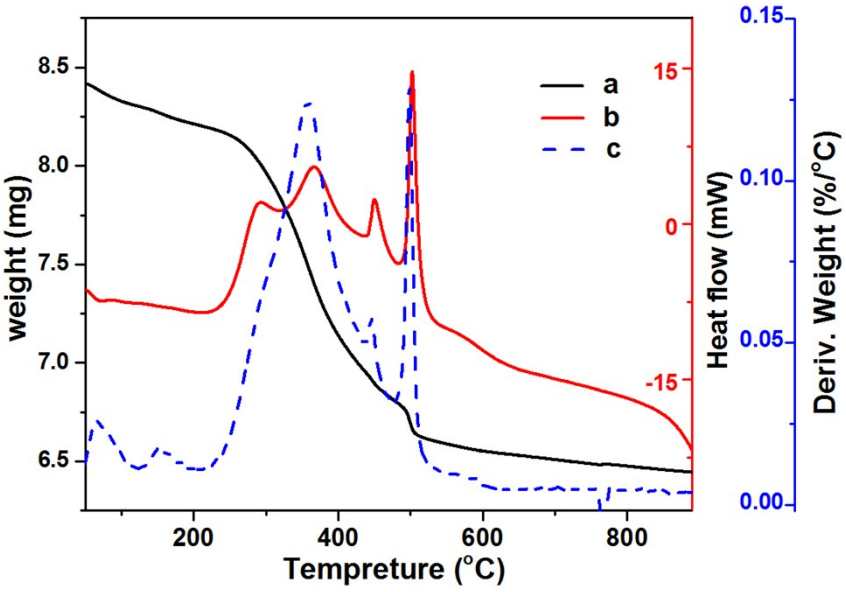

Fig. S21 (a) TG, (b) DTA and (c) DTG curves of Pt@MFI-a.

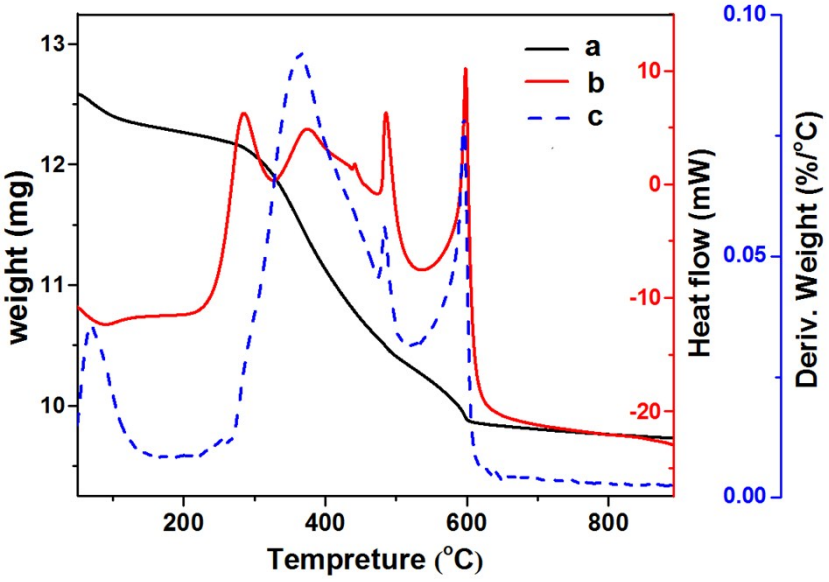

Fig. S22 (a) TG, (b) DTA and (c) DTG curves of Pt@MFI-b.

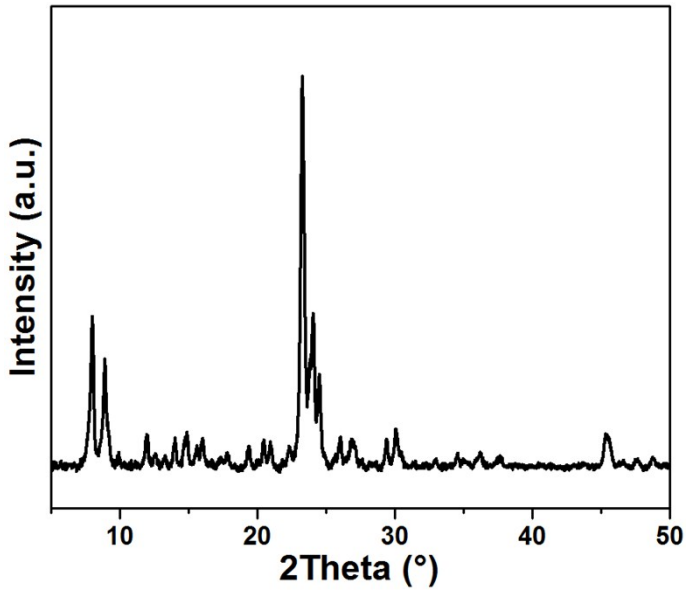

Fig. S23 XRD patterns of Ru@MFI after calcination at 500 °C.

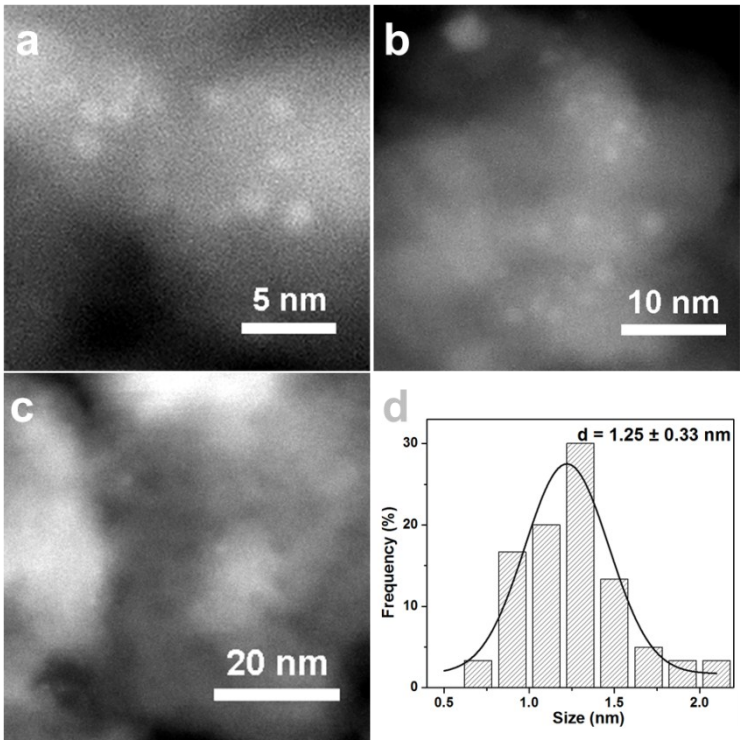

Fig. S24 STEM images of Ru@MFI after calcination at 500 °C under the scale bar of (a) 5 nm, (b) 10 nm, (c) 20 nm, (d) the particle size distribution.

Table S1 The ICP measurement results of the samples

Samples	Pt /wt.%	Al /wt.%
Pt@MFI-a	0.25	- [ND]
Pt@MFI-b	0.23	4.8

[ND] Not determined.

Table S2 BET surface areas and pore volumes of the samples

Samples	S_{BET} /$m^2\ g^{-1}$	S_{micro} /$m^2\ g^{-1}$	S_{meso} /$m^2\ g^{-1}$	V_{micro} /$cm^3\ g^{-1}$	V_{mecro} /$cm^3\ g^{-1}$	Medium pore width /nm
ZSM-5 seed	357	10	348	0.05	0.32	0.97
Pt@MFI-a	517	346	171	0.15	0.34	0.62
Pt@MFI-b	483	371	112	0.15	0.33	0.59

Table S3 The conversion of hydrogenation reactions over different catalysts

samples	$C_{3\text{-nitrotoluene}}$/%
Pt@MFI-b	58
Pt/ZSM-5-im	100